Cell Transplantation, Vol. 25, pp. 2083–2097, 2016

0963-6897/16 $90.00 + .00
DOI: http://dx.doi.org/10.3727/096368916X692069
E-ISSN 1555-3892
www.cognizantcommunication.com

Short-Term Grafting of Human Neural Stem Cells: Electrophysiological Properties and Motor Behavioral Amelioration in Experimental Parkinson's Disease

Alberto Martínez-Serrano,*† Marta P. Pereira,*† Natalia Avaliani,‡ Anna Nelke,*† Merab Kokaia,‡ and Tania Ramos-Moreno*†‡

*Department of Molecular Biology, Universidad Autónoma de Madrid, Madrid, Spain
†Department of Molecular Neurobiology, Center of Molecular Biology Severo Ochoa (UAM-CSIC), Madrid, Spain
‡Epilepsy Center/Stem Cell Center, Wallenberg Neuroscience Center, Lund University Hospital, Lund, Sweden

Cell replacement therapy in Parkinson's disease (PD) still lacks a study addressing the acquisition of electrophysiological properties of human grafted neural stem cells and their relation with the emergence of behavioral recovery after transplantation in the short term. Here we study the electrophysiological and biochemical profiles of two ventral mesencephalic human neural stem cell (NSC) clonal lines (C30-Bcl-X_L and C32-Bcl-X_L) that express high levels of Bcl-X_L to enhance their neurogenic capacity, after grafting in an in vitro parkinsonian model. Electrophysiological recordings show that the majority of the cells derived from the transplants are not mature at 6 weeks after grafting, but 6.7% of the studied cells showed mature electrophysiological profiles. Nevertheless, parallel in vivo behavioral studies showed a significant motor improvement at 7 weeks postgrafting in the animals receiving C30-Bcl-X_L, the cell line producing the highest amount of TH^+ cells. Present results show that, at this postgrafting time point, behavioral amelioration highly correlates with the spatial dispersion of the TH^+ grafted cells in the caudate putamen. The spatial dispersion, along with a high number of dopaminergic-derived cells, is crucial for behavioral improvements. Our findings have implications for long-term standardization of stem cell-based approaches in Parkinson's disease.

Key words: Human neural stem cells (hNSCs); Parkinson's disease (PD); A9-dopaminergic phenotype; Electrophysiology; Ventral mesencephalon

INTRODUCTION

Clinical research on cell replacement therapy (CRT) provided proof of principle of the therapeutic efficacy of dopaminergic transplants for Parkinson's disease (PD) on a long-term basis, using fresh human ventral mesencephalic (VM) tissue[1,2]. At present, human neural stem cells (hNSCs) and human induced pluripotent stem cells (hiPSCs) show great promise for CRT for neurological disorders[3]. Motor deficit amelioration has been reported for parkinsonian animals transplanted with human clonal neural stem cells in the short[4] and the long term[5]. It has been recently reported that, in long-term experiments, motor amelioration depends on previous graft integration and dopamine (DA) release of the transplanted human embryonic stem cells (hESCs) in the long term[6].

Nevertheless, little is known about the dynamics of how motor amelioration develops in the short term. In the present study, we analyze what DA-dependent variables may influence behavioral amelioration in parkinsonian models in the short term. For this, we used hVM-NSCs with different dopaminergic potentials, clones 30 and 32 (described in the study by Ramos-Moreno et al.[4]), that are forced to overexpress Bcl-X_L to maintain their neurogenic capacity[7]. hVM-NSC clones were grafted into an in vitro parkinsonian model to study their functional maturation and integration at 6 weeks, while hemiparkinsonian animals received both clones for in vivo behavioral and immunohistochemical analyses.

Our results show that the hVM-NSC cell derivatives display immature neuronal properties in the short term—6 weeks postgrafting. However, out of 45 total recorded cells, 1 C30-Bcl-X_L- and 2 C32Bcl-X_L-derived cells showed mature neuronal electrophysiological profiles, one of them fitting with the reported dopaminergic

Received March 20, 2016; final acceptance September 13, 2016. Online prepub date: June 17, 2016.
Address correspondence to Tania Ramos-Moreno, Ph.D., Glioma Cell Therapy Group, Lund Stem Cell Center, Division of Neurosurgery/ Department of Clinical Sciences, Lund University, BMC B10, SE-221 84 Lund, Sweden. Tel: +46 46 222 31 59; Fax: +46 46 2220560; E-mail: tania.ramos_moreno@med.lu.se

firing. Despite the immature electrophysiological profile of the majority of in vitro-examined cells at this time point, parkinsonian animals transplanted with the C30-Bcl-X_L clone undergo a behavioral amelioration. Histological analyses confirmed the presence of integrated human tyrosine hydroxylase (TH^+) cells derived from both transplanted cell lines in the striatum and the coexpression of markers for neuronal maturation such as Map2ab and vesicular monoamine transporter 2 (VMAT2). The correlation analysis shows that behavioral amelioration depends mostly on the extent of the caudate putamen that might be exposed to DA release from the transplant.

MATERIALS AND METHODS

Ethics Statement

Principles of both research with laboratory animals and use of stem cells were approved by the relevant research ethics committees: Autonomous University Committee for Research Ethics (permit CEI 23-564), *Comisión de Seguimiento y Control de la Donación y Utilización de Células y Tejidos Humanos* (permit 123-101-1), and *Comité Regional Ético de Investigación Clínica de la Consejería de Sanidad de la Comunidad de Madrid* (permit OPTISTEM-DA). Additional ethics statements about the human fetal origin of the cells used in the present study can be found in the original reports describing the generation of the parental hVM1 and hNS1 cell lines used here[8–10]. Use of animals for organotypical slice cultures was approved by the Lund/Malmö Ethics Committee (permit M204-12). All animal work was designed following the 3Rs principles. Experiments were carried out according to the guidelines of the European Community (directives 86/609/ECC and 2010/63/EU). Details of animal work and welfare are described under the Animal Experimentation section below.

Cell Culture Procedures

The cells used in the present study were perpetuated with v-*myc* and include a Bcl-X_L-overexpressing hVM cell line (hVM1-high Bcl-X_L)[7,8], used as a parallel control for present studies, and the two clonal derivatives of the parental hVM1 C30 and C32[4,8] Bcl-X_L-overexpressing parallel lines (from here on designated as C30-Bcl-X_L and C32-Bcl-X_L, respectively). Briefly, to generate the stable C30-Bcl-X_L and C32-Bcl-X_L, clones C30 and C32 were transfected with a Bcl-X_L-coding plasmid (LTR-Bcl-X_L-IRES-hrGFP-LTR)[7,10] using Lipofectamine 2000 (Invitrogen, Thermo Fisher Scientific, Madrid, Spain), when their passage numbers were 16 and 22, respectively. C30-Bcl-X_L^+ and C32-Bcl-X_L^+ cells were sorted using a fluorescence-activated cell sorter, the FACSCalibur flow cytometer (BD Biosciences, Madrid, Spain) as previously described[7]. Bcl-X_L overexpression was also confirmed by Western blot four passages later (data not shown).

Cells were routinely cultured on 10 μg/ml poly-L-lysine-pretreated plastic ware in recombinant human epidermal growth factor (EGF) and basic fibroblast growth factor (bFGF) (20 ng/ml each; R&D Systems, Minneapolis, MN, USA)-supplemented chemically defined medium (referred to hereafter as "proliferation medium")[4,8]. Cells were grown at 37°C, in 95% humidity, 5% CO_2, and 5% O_2 atmosphere (normoxic conditions for brain tissue) in a dual CO_2/O_2 control incubator (Forma; Thermo Fisher Scientific). Alternatively, for the immunocytochemistry assays, the cells were grown on poly-L-lysine-pretreated, glass coverslips. Cells were differentiated in differentiation medium [proliferation medium without mitogens EGF or bFGF and enriched with 2 ng/ml glial cell line-derived neurotrophic factor (GDNF; PeproTech, London, UK) and 1 mM dibutyryl cyclic adenosine monophosphate (db-AMPc; Sigma-Aldrich, Madrid, Spain)[11]].

Immunocytochemistry (ICC)

Cultures were fixed under proliferation conditions or after 10 days of differentiation with 4% buffered paraformaldehyde (PFA; Sigma-Aldrich). Cells on coverslips were incubated overnight at 4°C in 1× phosphate-buffered saline (PBS) containing 1% goat serum (Gibco; Thermo Fisher Scientific) and 0.25% Triton X-100 (Sigma-Aldrich) with the primary monoclonal antibodies anti-Ki-67 (1:200; Thermo Fisher Scientific) or anti-β-III-tubulin (1:2,000; Sigma-Aldrich) and primary polyclonal antibody against TH (1:1,000; Chemicon, Merck Chemicals and Life Science GesmbH, Madrid, Spain). Samples were washed and incubated afterward for 1 h with appropriate fluorescent secondary antibodies: Cy5-conjugated donkey anti-rabbit (1:200; Jackson ImmunoResearch, Suffolk, UK), Cy3-conjugated goat anti-mouse (1:200; Jackson Immuno Research), and counterstained with Hoechst 33342 (1:400; Life Technologies, Thermo Fisher Scientific) to label nuclei.

In Vitro Cell Quantification and Microscopy Analysis of C30-Bcl-X_L and C32-Bcl-X_L Cultures

In vitro quantification of cell numbers was done in triplicate samples (coverslips) per condition (differentiated vs. proliferating states) in a Leica DM IRB epifluorescence microscope equipped with a digital camera Leica DC100 (Nussloch, Germany). In some of the immunofluorescence experiments, digital images were captured using Leica IM500 or LSM710 software. Image analyses were performed using the National Institutes of Health (NIH; Bethesda, MD, USA) ImageJ software. The total number of cells in each region of interest was counted using Hoechst 33342 nuclear counterstaining.

Organotypic Striatal Cultures and Cell Coculture

Organotypic cultures were prepared as 250-µm-thick coronal hemisphere sections of postnatal days 6–8 BALB/c mice. After decapitation, brains were removed and each hemisphere was embedded in physiological agar to offer mechanical support while slicing coronal sections at 4°C in modified artificial cerebrospinal fluid (aCSF) containing 195 mM sucrose, 2.5 mM KCl, 1.25 mM NaH_2PO_4, 28 mM $NaHCO_3$, 0.5 mM $CaCl_2$, 1 mM L-ascorbic acid, 3 mM pyruvic acid, 7 mM glucose, and 7 mM $MgCl_2$ (all from Sigma-Aldrich) equilibrated with 5% CO_2 in oxygen. Sections were selected to include striatum and the overlying cortex. After slicing, sections were kept in ice-cold washing medium containing Hank's balanced salt solution (HBSS) with 20 mM 4-(2-hydroxyethyl)-1-piperazineethanesulfonic acid (HEPES), 17.5 mM glucose, 0.88 mM NaOH, and 1% penicillin/streptomycin (all from Gibco; Thermo Fisher Scientific, Waltham, MA, USA) for 15 min before placing individual slices on membrane inserts (PICM01250; Millipore, Merck Chemicals and Life Science GesmbH, Stockholm, Sweden) in 240 µl of cell culture medium in 12-well plates. The culturing medium contained 50% minimum essential medium (MEM), 25% horse serum, 18% HBSS, and 2% B27, supplemented with 0.5% penicillin/streptomycin, 2 mM glutamine (all from Life Technologies, Thermo Fisher Scientific), 11.8 mM glucose, 20 mM sucrose, 30 ng/ml brain-derived neurotrophic factor (BDNF; R&D Systems), 30 ng/ml GDNF (R&D Systems), and 0.2 mM L-ascorbic acid. Slices were cultured as interface cultures at 37°C, 5% CO_2, and 90% humidity. Medium was changed on day 1 of culturing and three times per week thereafter. B27 was withdrawn from the medium after 1 week. In vitro grafting was performed on day 1 after slice cultures had been prepared. Prior to micrografting, C30-Bcl-X_L, C32-Bcl-X_L, and hVM1-Bcl-X_L cells were trypsinized (Gibco; Thermo Fisher Scientific), spun down at $890 \times g$, and resuspended in Ca^{2+}- and Mg^{2+}-containing HBSS (Invitrogen, Thermo Fisher Scientific) to reach a concentration of 5×10^3cells/µl. Between 10,000 and 15,000 cells were placed on the striatal region of each slice using an Eppendorf micropipette (Eppendorf Nordic A/S, Hoersholm, Denmark). Coculturing conditions were as described above for organotypic cultures (for more information see Tonnesen et al.[12]).

Electrophysiology

After 6 weeks in coculture, the electrophysiological properties of grafted clones that were green fluorescent protein-positive (GFP^+) cells in the slices and all Bcl-X_L cells that also express *Renilla raniformis* humanized GFP were assessed as previously described[12]. Slice cultures were transferred on their culturing membrane to a recording chamber continuously perfused at 4 ml/min with aCSF containing 119 mM NaCl, 2.5 mM KCl, 1.3 mM $MgSO_4$, 2.5 mM $CaCl_2$, 26.2 mM $NaHCO_3$, 1 mM NaH_2PO_4, and 11 mM glucose (300 mOsm, pH 7.4; all from Sigma-Aldrich) at 32.5°C. For whole-cell patch-clamp recordings, a pipette solution containing 122.5 mM K-gluconate, 17.5 mM KCl, 8 mM NaCl, 10 mM KOH-HEPES, 0.2 mM KOH-EGTA, 2 mM MgATP, and 0.3 mM Na_3GTP (295 mOsm, pH 7.2; all from Sigma-Aldrich) was used, yielding a tip resistance of 3–6 MΩ. Biocytin (Biotium, Fremont, CA, USA) was included in the pipette solution at 0.5–1 mg/ml to retrospectively identify recorded neurons. GFP-expressing cells were visualized using a wide-band excitation filter (420–480 nm), and whole-cell and patch-clamp recordings were made using infrared differential interference contrast video microscopy (BX50WI; Olympus Sverige AB, Stockholm, Sweden).

Resting membrane potential (RMP) was recorded in current clamp mode at 0 pA immediately after establishing the whole-cell configuration, while postsynaptic currents were recorded in voltage clamp mode holding the RMP at −70 mV. Rectification and action potential threshold were determined from stepwise de- or hyperpolarization of the membrane potential by injecting positive or negative square current pulses for 0.5 s at 20- to 40-pA increments from RMP (0 pA). Step current depolarizations were used to determine the action potential threshold. Duration of afterhyperpolarization following action potentials was measured as the entire duration of the membrane potential below RMP immediately following action potentials. All currents and voltages were registered and controlled using a HEKA EPC10 amplifier (HEKA Elektronik, Lambrecht/Pfalz, Germany). Mini Analysis software (Synaptosoft Inc., Fort Lee, NJ, USA) was used for detection and analysis of spontaneous postsynaptic currents. Their rise time was measured as the time between 10% and 90% of the maximum amplitude, while the decay time was first fitted with a single exponential and then measured as above.

Animal Experimentation: Lesion, Drug-Induced Rotation, and Transplantation Procedures

Animals used in this study were 3-month-old female Sprague–Dawley rats (Harlan Laboratories, Barcelona, Spain) weighing 200–250 g at the beginning of the experiment. Animals were housed in a temperature- and humidity-controlled room, under a 12 h-light/dark cycle, with ad libitum access to food and water. Rats received a 3-µl injection of 6-hydroxydopamine (6-OHDA) (9 µg 6-OHDA in 0.2 mg/ml ascorbic acid in saline; Sigma-Aldrich) in the right medial forebrain bundle at the following stereotaxic coordinates (tooth bar set at −3.3 mm): anteroposterior, −3.7 mm (from bregma); mediolateral, −1.6 mm (from bregma); and dorsoventral, −8.8 mm

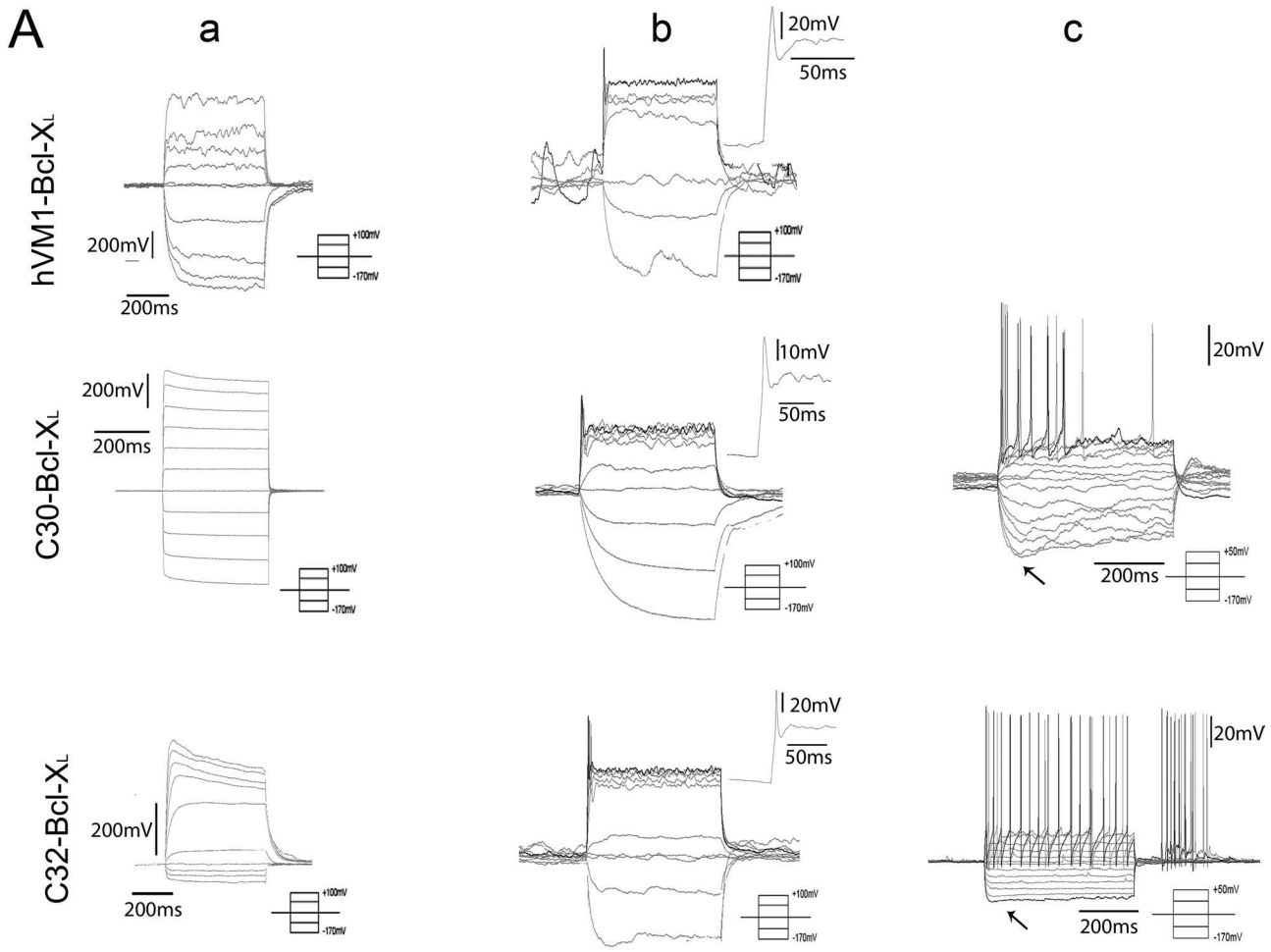

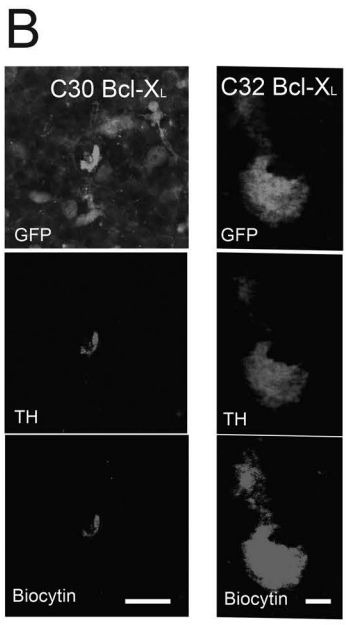

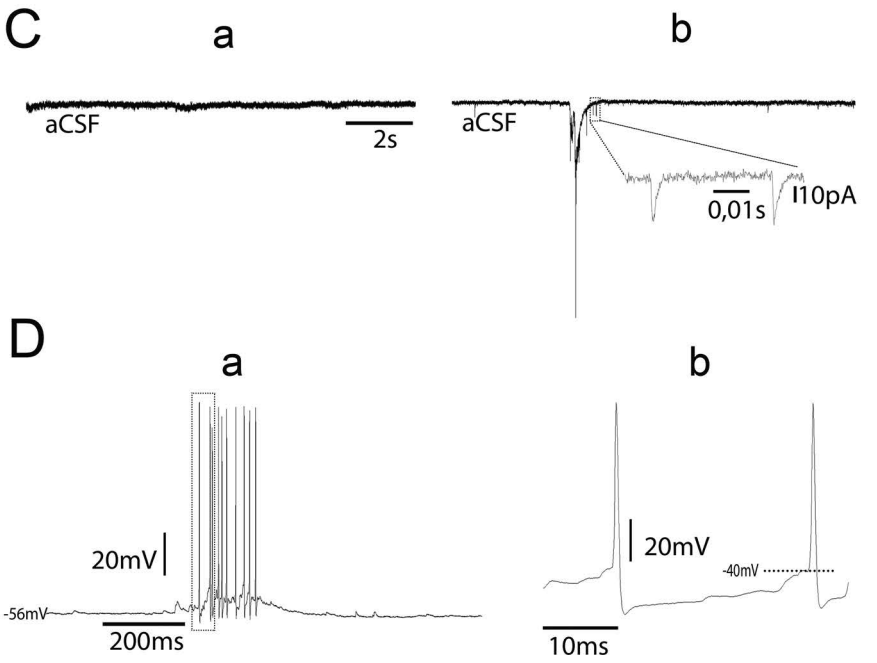

(from dura). The injection rate was 1 µl/min, and the needle was kept in place for an additional 5 min before being slowly retracted. Four weeks after the lesion, the rats were tested for drug-induced rotational behavior in automated rotometer bowls (Panlab S.L.U., Barcelona, Spain) following an intraperitoneal (IP) injection of D-amphetamine sulfate (5 mg/kg; Sigma-Aldrich). Rotation scores were collected every 2 min for 90 min in a computer-assisted rotometer system (Panlab). Only rats exhibiting five or more ipsilateral rotations/min after D-amphetamine injection were selected for transplantation studies. After balancing the experimental groups (7–10 animals per group), the hemiparkinsonian rats were transplanted with cells in proliferative state. Cells were trypsinized (Gibco; Thermo Fisher Scientific) and resuspended in Ca^{2+}- and Mg^{2+}-containing HBSS (Invitrogen, Thermo Fisher Scientific) at densities of 10^5/µl. Cell suspensions (3 µl, a total of 3×10^5 cells per deposit) were injected into the denervated striatum in a single track and deposited at the following coordinates (tooth bar set at −2.3): anteroposterior, +1 mm (from bregma); mediolateral, −3 mm (from bregma); and dorsoventral, −4.5 mm (from dura). The animals were immunosuppressed with daily IP cyclosporin A injection (15 mg/kg; Novartis, Barcelona, Spain) starting 2 days before transplantation and throughout the experiment. A few animals in this experiment were allowed to survive for 12 weeks to study the glial scar surrounding the cell bolus. Since animals transplanted with polyclonal hVM1-high Bcl-X_L cells have been previously reported not to show behavioral amelioration at short-term postgrafting[4,5], and the use of clones has been reported to be more effective and suitable for preclinical studies[4], only C30-Bcl-X_L and C32-Bcl-X_L were used for transplantation.

Immunohistochemistry (IHC)

Seven weeks after transplantation, the animals were sacrificed with an overdose of chloral hydrate and intracardially perfused with 4% PFA (in 0.1 M phosphate buffer, pH 7.4). Brains were removed, postfixed for 12 h in the same fixative at 4°C, and dehydrated in 30% sucrose solution at 4°C until they sunk. Ten series of 30-µm-thick coronal sections were collected using a freezing microtome (Leica Biosystems, Bromma, Sweden). Serial free-floating sections were incubated overnight at 4°C in PBS containing 1% goat serum and 0.25% Triton X-100 with the following primary antibodies: polyclonal anti-glial fibrillary acidic protein (GFAP) (1:1,000; Dako, Agilent, Santa Clara, CA, USA), ionized calcium-binding adaptor molecule 1 (Iba-1) (1:1,200; Wako Chemicals GmbH, Neuss, Germany), and TH (1:400; Pel-Freez, Rogers, AR, USA), and monoclonal antibodies against human nuclei (HuNu) (1:100; Chemicon, Merck Chemicals and Life Science GesmbH), Ki-67 (1:200; Thermo Fisher Scientific), VMAT2 (1:500; Chemicon, Merck Chemicals and Life Science GesmbH); Map2ab (1:1,000; Thermo Scientific Pierce Antibodies, Thermo Fisher Scientific), 4′,6-diamidino-2-phenylindole (DAPI; 1:1,000; AnaSpec, Fremont, CA), human cytoplasmic marker sc-121 (1:500; Takara Laboratories, Madrid, Spain), and antibody specific for human GFAP sc-123 (1:500; Takara Laboratories). Sections were washed and incubated for 1 h with appropriate secondary antibodies, biotinylated goat anti-rabbit (1:200; Vector Laboratories, Burlingame, CA, USA), biotinylated rabbit anti-sheep (1:200; Vector Laboratories), Cy5-conjugated donkey anti-mouse (1:200; Jackson ImmunoResearch), and Cy3-conjugated goat anti-rabbit (1:200; Jackson Immuno Research). The biotinylated sections were then incubated with an avidin–biotin–peroxidase complex (ABC Kit; Vector Laboratories) and developed with 1,3-diaminobenzidine (DAB; Sigma-Aldrich) or VIP reagent (Vector Laboratories). Finally, all sections were mounted onto gelatinized glass slides (Menzel-Glaser; Thermo Fisher Scientific), dried overnight, mounted with Mowiol (Calbiochem, Merck Chemicals and Life Science GesmbH), and coverslipped.

FACING PAGE

Figure 1. Polyclonal hVM-Bcl-X_L cells and clones 30-Bcl-X_L and 32-Bcl-X_L were grafted into organotypic cultures, a model for PD[12], and allowed to mature for 6 weeks, at which point their electrophysiological properties were studied. Action potentials (APs) were induced upon 5- and 10-pA increments of current step injection 6 weeks after grafting. (A) Attending to their AP firing, the following maturational stages were recorded: completely immature (a), immature APs (b), and mature APs (c). Note that no mature APs were recorded for the hVM-Bcl-X_L cell line, probably due to a low probability of finding such cells, as the majority of cells are immature. The frequency of firing in column c (15 Hz) and sag component (arrows) are characteristic of dopaminergic firing patterns upon stepwise depolarization current injection[19]. (B) Column on the left shows 1-µm-thick confocal image of the patched GFP-expressing C30-Bcl-X_L cell stained for TH. This cell showed immature APs upon stepwise depolarization currents (traces represented in Ab). Scale bar: 20 µm. Column on the right shows 1-µm-thick confocal image of the recorded GFP-expressing grafted C32-Bcl-X_L cell stained for TH. Its correspondent trace is represented in Ac showing mature DA electrophysiological profile. Both morphologies resemble the DA morphology described for TH^+ cells in substantia nigra (reported in Grace and Onn[13]). Arrows point to an axonal process. Scale bar: 5 µm. (C) Spontaneous postsynaptic events (a) corresponding to a completely immature hVM-Bcl-X_L cell (Aa) and (b) corresponding to the C32-Bcl-X_L showing mature APs (Ac, B). Note the spontaneous discharge in (D). Whole-cell recordings in current-clamp mode of the C32-Bcl-X_L cell shown in (Ac) and the right column in (B). (a) Characteristic dopaminergic spontaneous 1- to 10-Hz trains of firing can be observed. Spikes in boxes are shown in more detail in (b), where the AP threshold and the slow membrane depolarization can be observed.

Quantification and Microscopical Analysis of the Grafted Cells Into the Striatum In Vivo

The total number of $HuNu^+$, Ki-67^+, and TH^+ cells in the graft was stereologically determined using CAST Grid software (Visiopharm, Hoersholm, Denmark) in three animals randomly taken per group. For colocalization of HuNu and Ki-67 antibodies, around 500 cells per animal were counted in random fields from the graft area in an epifluorescence microscope (Olympus BX61; Olympus Sverige AB; Solna, Stockholm, Sweden).

Results were expressed as percentage of total number of Ki-67^+ cells. TH^+ cell counting and morphology were assessed in the same animals. Colocalization of different markers was validated using a confocal microscope (Leica).

The same three animals per group underwent optical density (OD) measurements, at three to four fields at 10× magnification per slice covering the entire caudate putamen, from its appearance in the anterioposterior axis until the appearance of the third ventricle. The software ImageJ was used for the area quantification and OD. Pictures of substantia nigra at the same levels were measured for determining the lesion.

Data Analysis

All behavioral testing was conducted by investigators blind to the treatments of the rats. Statistical analysis was used to compare groups for signed rank test with a significance level of $p<0.05$.

Analysis of electrophysiological data was performed using Fitmaster (HEKA Elektronik) and Igor Pro (Wavemetrics, Portland, OR, USA). A one-tailed Student's *t*-test was applied to analyze differences in the electrophysiological properties and number of Ki-67^+ cells of the hVM1-Bcl-X_L, C30-Bcl-X_L, and C30-Bcl-X_L grafted cells. The level of significance was $p\leq0.05$. All data are presented as mean ± standard error of the mean (SEM). Correlation analysis of the OD and cell counting was performed using StatPlus:mac version 6 (AnalysisSoft Inc., Walnut, CA, USA).

RESULTS

Electrophysiological Maturation and Synaptic Integration of the Genetically Modified Human Clones After Grafting

C30-Bcl-X_L and C32-Bcl-X_L cells were grafted onto striatal coronal slices, which can be considered as an in vitro model of PD[12], and cocultured for 6 weeks to study the functional properties, maturation, and integration of the hVM-NSC clones after transplantation.

Most of the grafted hVM-NSCs displayed immature neuronal properties 6 weeks postgrafting. A total of 42 cells showed either no action potentials (APs) or immature APs upon stepwise depolarization by current injection (Fig. 1A and Table 1). However, relatively mature APs were recorded in one C32-Bcl-X_L cell, which is documented to be a transplanted cell with biocytin diffused from the recording pipette (Fig. 1Ac and B) and in two other cells (one C30-Bcl-X_L cell and one C32-Bcl-X_L cell), visually confirmed for GFP expression during the electrophysiological recording. Out of these three cells, the two cells belonging to the C32-Bcl-X_L group showed spontaneous firing in current-clamp mode, and one of them showed a low-frequency regular AP firing activity (Fig. 1D). The profile also included broad APs followed by a pronounced afterhyperpolarization and a "sag" component induced by step current hyperpolarization, all characteristic for midbrain nigral DA neurons[13–15] (see Fig. 1Ac).

RMPs and input resistance (Ri) data for recorded cells are shown in Table 1. RMPs were −61.4 ± 3.3 mV for the hVM1-Bcl-X_L cells, −48.96 ± 6.07 mV for the C30-Bcl-X_L cells, and −56.64 ± 3.67 mV for the C32-Bcl-X_L cells. Ri values were 1,990 ± 478 MΩ for the hVM1-Bcl-X_L cells, 1,487.48 ± 393 MΩ for the C30-Bcl-X_L cells,

Table 1. Electrophysiological Properties of the 45 Different hVM1 Cell-Derived Neurons at 6 Weeks Postgrafting in Organotypical Striatal Slices

Immature (42 Cells)			Mature (3 Cells)			
hVM1-Bcl-XL	C30-Bcl-XL	C32-Bcl-XL	hVM1-Bcl-XL*	(1) C30-Bcl-XL	(2) C32-Bcl-XL	
1,990 ± 478	1,487.48 ± 393	1,500.39 ± 386.76	–	396.19	424.24 ± 312	Ri (MΩ)
−61.40 ± 3.3	−48.96 ± 6.07	−56.64 ± 3.67	–	−52.4	−58.28 ± 11.77	RMP
−4.62 ± 7.19	−10.13 ± 5.11	−17.82 ± 9.09	–	−38.26	−36.23 ± 5.89	AP thresh (mV)
27.19 ± 11.91	21.33 ± 5.49	45.36 ± 12.96	–	80.91	71.41 ± 1.40	AP ampl (mV)
11.25 ± 6.31	5.63 ± 1.91	2.61 ± 0.91	–	1.3	1.27 ± 1.15	AP ½ dur (ms)
5.25 ± 3.98	0.70 ± 3.74	11.20 ± 3.35	–	11	14.04 ± 7.67	AHP (mV)

*No electrophysiologically mature cell was recorded for hVM1-Bcl-X_L. (1) Only one of the recorded neurons derived from the C30-Bcl-X_L cells showed APs. (2) Two of the recorded neurons derived from the C32-Bcl-X_L cells showed APs. Please note the AP threshold (around −40 mV) and the high AP amplitudes and AHP values, characteristic of dopaminergic neurons when recorded in vivo in rats[13,19]. Data are presented as mean ± standard error of the mean (SEM). AP, action potential, AHP, afterhyperpolarization.

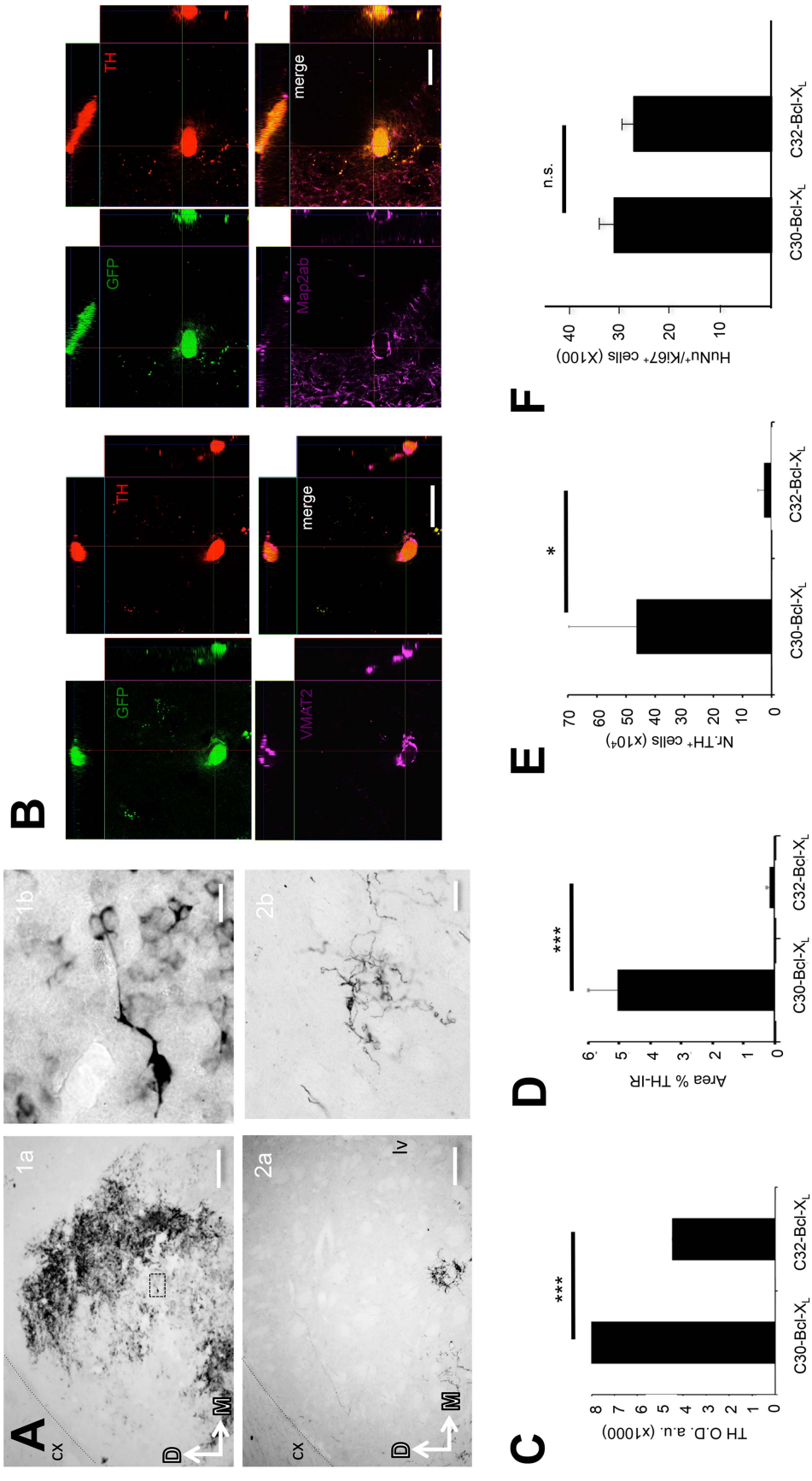

Figure 2. Histology supports the results obtained in the drug-induced behavioral test. (A) (1a) Representative TH expression in a grafted striatum receiving C30-Bcl-X_L cells 7 weeks after grafting. Scale bar: 100 μm. (1b) Magnifications of the grafted cells boxed in the left microphotograph are shown. Scale bar: 10 μm. cx, cortex. (2a) Representative TH expression in a grafted striatum receiving C32-Bcl-X_L cells 7 weeks after grafting. Scale bar: 100 μm. (2b) Magnifications of the grafted cells boxed in the left microphotograph are shown. Scale bar: 20 μm. cx, cortex; Lv, lateral ventricle; D, dorsal; M, medial. (B) Clone 32-Bcl-X_L-derived cells express markers of neuronal maturation 7 weeks postgrafting (1-μm-thick confocal images). Left: Colocalization of TH with VMAT2. Right: TH colocalizing with Map2ab. Scale bars: 10 μm. (C) Optical density (OD) values for TH immunoreactivity (TH-IR) throughout the caudate putamen. a.u., arbitrary units. Data are expressed as the mean ± SEM; 71,837.34 ± 2.3 and 4,479.02 ± 0.31 for C30-Bcl-X_L and C30-Bcl-X_L, respectively. ***$p < 0.001$, Student's *t*-test; $n = 3$. (D.) Percentage (%) of the caudate putamen immunoreactive to TH. Data are expressed as the mean ± SEM; 5.05 ± 0.93 and 0.18 ± 0.09 for C30-Bcl-X_L and C30-Bcl-X_L, respectively. ***$p < 0.001$, Student's *t*-test; $n = 3$. (E) Number of TH^+ surviving cells for C30-Bcl-X_L and C32-Bcl-X_L at 7 weeks postgrafting. 462,741.67 ± 233,802.38 and 24,880.95 ± 22,219.28 for C30-Bcl-X_L and C30-Bcl-X_L (mean ± SEM). $p \leq 0.05$, Student's *t*-test; $n = 3$. (F) Graph combining the data for the C30-Bcl-X_L and C32-Bcl-X_L for the percentage of human cells ($HuNu^+$ cells) coexpressing Ki-67 at 7 weeks postgrafting. 30.76 ± 6.55 and 29.51 ± 1 for C30-Bcl-X_L and C30-Bcl-X_L. Data are expressed as the mean ± SEM; n.s., nonsignificant; Student's *t*-test; $n = 3$.

and 1,500.39 ± 386.76 MΩ for the C32-Bcl-X_L cells. No statistical significance was observed between the groups.

Spontaneous postsynaptic currents (sPSCs) recorded at −70 mV in whole-cell voltage-clamp mode showed that out of the 45 recorded hVM1 cell-derived neurons recorded, 7 cells [1 hVM1-Bcl-X_L cell, 2 C30-Bcl-X_L cells (1 immature and 1 mature firing profile) and 4 C32-Bcl-X_L cells (2 immature and 2 mature firing profiles)] displayed sPSCs 6 weeks after grafting. Cells were first identified under the microscope by their GFP expression, and four could be later confirmed with biocytin (one hVM1-Bcl-X_L, one immature C30 Bcl-X_L, one immature C32 Bcl-X_L, and one mature C32 Bcl-X_L).

Immunohistochemical and Quantitative Studies of hVM1 C30-Bcl-X_L and C32-Bcl-X_L Cell Grafts In Vivo

Our data show that while some of the ex vivo-grafted cells may express TH but do not fire any AP, all cells with characteristic DA AP firings are TH immunoreactive (Fig. 1B).

IHC confirmed graft survival and cytoarchitectural integration in the recipient tissue in the in vivo short-term studies (7 weeks postgrafting). The grafts' appearance was rounded and rather compact, similar to that shown by human and rodent fresh VM tissue grafts, containing many TH^+ cells located around the injection site in the striatum for C30-Bcl-X_L (Figs. 2A and 3E–G). Animals receiving C30-Bcl-X_L showed a better production of TH^+ cells and a higher TH^+ immunoreactivity extension when compared to C32-Bcl-X_L grafts (Fig. 3E). OD measurements of the TH stain between groups revealed statistical differences. OD values were 71,837.34 ± 2.3 and 4,479.02 ± 0.31 arbitrary units for C30-Bcl-X_L and C30-Bcl-X_L, respectively. Extension of the percentage of the area being reactive to TH was 5.05 ± 0.93 and 0.18 ± 0.09 for C30-Bcl-X_L and C30-Bcl-X_L, respectively (data expressed as the mean ± SEM; $p < 0.001$) (Fig. 2C and D). No difference in OD measured in the region of the substantia nigra between analyzed cases was observed (data not shown). In addition, stereological cell counting also showed significance for the TH^+ surviving cells between grafted groups (Fig. 2D). Specifically, TH-immunoreactive cell numbers were 462,741.67 ± 233,802.38 and 24,880.95 ± 22,219.28 cells per transplant for C30-Bcl-X_L and C30-Bcl-X_L (mean ± SEM; $p \leq 0.05$).

Both C30-Bcl-X_L- and C30-Bcl-X_L-derived cells showed expression of VMAT2 and Map2ab (Fig. 2B). In addition, both hVM-NSC clone transplants contain similar percentage of Ki-67^+ cells in the grafts, 30.76 ± 6.55 and 29.51 ± 1 for C30-Bcl-X_L and C30-Bcl-X_L, respectively (Fig. 2F). Finally, the human cytoplasmic marker sc-121 immunostaining denotes a similar survival rate between grafted animals (Fig. 3F).

Glial Reactivity Surrounding the Graft Core

The glial scar surrounding the graft core ($HuNu^+$ cells) shows GFAP Iba-1^+ cells vastly protruding into the transplanted cell bolus (Fig. 4A and B). Within the graft, few macrophages can be detected by hemosiderin deposits like those in the needle track of sham-operated animals. Glial response is also detectable further from the graft core (1.7 mm medial) but comparable to that on nontransplanted animals, indicating that it is not a specific glial response toward the grafted cells. Migrating

FACING PAGE

Figure 3. (A) Graph shows amphetamine-induced rotation counts pregrafting and 7 weeks following in vivo transplantation. Animals grafted with the naive clones behave as previously described[5]. Animals receiving C30-Bcl-X_L cells show a significant improvement of their rotational asymmetry (*$p \leq 0.05$, Wilcoxon signed rank test, two tailed; *$p < 0.05$, Student's *t*-test; $n = 7–10$). Data are expressed as the mean ± SEM. (B) Correlation between drug-induced behavior in transplanted animals with C30-Bcl-X_L and TH^+ cell numbers in the caudate putamen at 7 weeks postgrafting ($R = 0.77$; $p = 0.08$). (C) Correlation between OD for TH staining in the transplanted striatum and TH^+ cell numbers in the caudate putamen at 7 weeks postgrafting. Rat transplanted with the C30-Bcl-X_L cell line ($R = 0.88$; $p = 0.3$). (D) Correlation between drug-induced behavior in transplanted animals with C30-Bcl-X_L and OD for TH cell numbers in the caudate putamen at 7 weeks postgrafting ($R = 0.97$; $p = 0.059$). (E) (a, b) Representative striatal-level sections from animals grafted with C30-Bcl-X_L cells, showing high (a) and low (b) numbers of graft-derived TH^+ cells. Scale bars: 1 mm. Box 1 in (a) shows the high presence of TH^+ cellularity of the transplant. Scale bar: 40 μm. Box 2 in (a) shows morphologically mature TH^+ cell showing processes sprouting from the soma. Arrow points at the axon. Scale bar: 50 μm. Box 1 in (b) is the magnification showing the immature morphology often seen in the TH^+ cells derived from the grafted C30-Bcl-X_L cells. Scale bar: 50 μm. (c) Representative TH IHC of C32-Bcl-X_L cell-grafted rat brains revealing a scant presence of TH^+ cells and a more abundant presence of striatal TH^+ fibers at 7 weeks postgrafting. Scale bar: 1 mm. Boxes 1 and 2 in (c) show the prevailing presence of TH^+ striatal fibers in contrast to a scarce presence of TH^+ cells (box 2 shows solely the presence of TH^+ cells in the section). Scale bars: 100 μm (box 1), 20 μm (box 2). (d) Same case as in (c) at a more posterior level, where only TH^+ striatal fibers can be observed. 1 indicates magnification of the box in (e) showing TH^+ striatal fibers at a bigger magnification. Scale bar: 100 μm. (e) Immunofluorescence detecting HuNu in a consecutive section of the brain section shown in (c) and (d) that confirms presence of grafted C32-Bcl-X_L cells. Scale bars: 1 mm (c–e). (F) Representative photomicrographs for striatal brain sections from rats transplanted with C30-Bcl-X_L and C32-Bcl-X_L. Transplanted cells show good survival as shown by the human cytoplasmic marker sc-121 7 weeks postgrafting. Scale bar: 1 mm. (G) A fraction of the grafted cells shows typical astrocytic morphology accompanied by intense GFAP expression, indicating some cells of the surviving population become mature astrocytes. Scale bars: 1 mm and 100 μm in the magnification. Cx, cortex; Str, striatum; Ac, accumbens nucleus; LV, lateral ventricle.

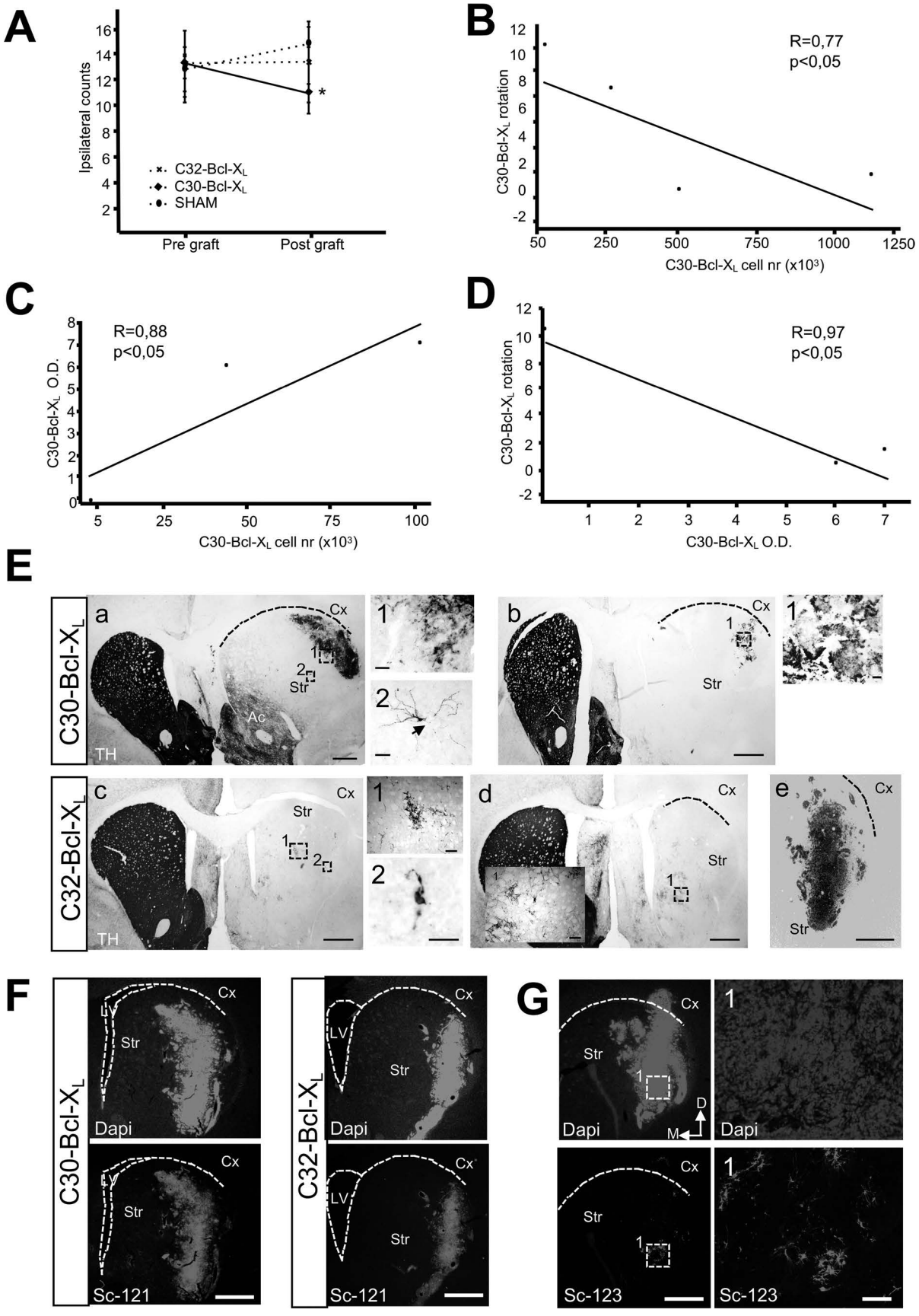

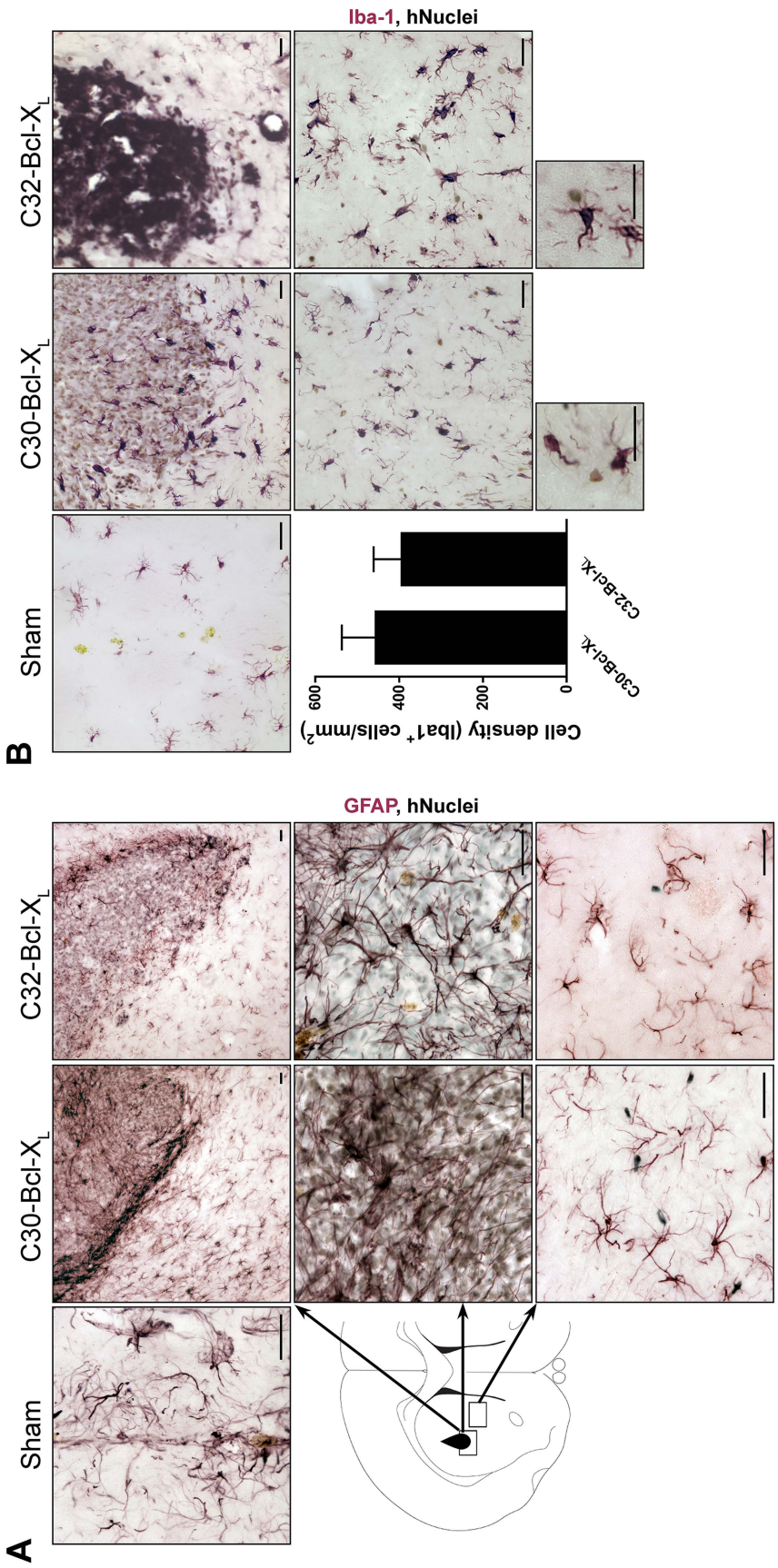

Figure 4. Glial markers around the transplanted cells. (A) There is dense astrocytic scar surrounding the transplanted cells with cytoplasmic elongations protruding in the cell bolus. Found 1.7 mm from the cell bolus astrocytes are accompanying migrating hNSCs through the host's parenchyma. (B) Similarly to astrocytes, activated microglia surround the transplanted cell bolus and the migrating cells in the host's striatum. Scale bars: 25 μm.

hNSCs (particularly C30- Bcl-X_L cells) show a close relationship with the host's astrocytes and microglia (Fig. 4, high-magnification insets). It is worth noting that glia derived from the transplants seems to be present at low numbers (Fig. 3G).

Behavioral Amelioration In Vivo

Amphetamine-induced rotation tests were carried out for all animal groups prior to transplantation and at 7 weeks postgrafting. Only animals receiving C30-Bcl-X_L cells showed a significant reduction of drug-induced rotation ($p<0.05$) (Fig. 3A). C30-Bcl-X_L cells are the ones producing more TH^+ cells after differentiation both in vitro and in vivo, these covering a higher extent of the caudate putamen (Figs. 2A, 3E, and 5C).

Data regarding OD measurements and cell counting were subsequently subjected to a linear regression analysis for behavioral improvement. Although there is a possible correlation between the TH^+ cell numbers and the behavioral improvement ($R=0.77$) (Fig. 3B), the strongest correlation associated to the behavioral improvement is the extension of the caudate putamen covered by the TH^+ surviving cells ($R=0.97$) (Fig. 3D).

DISCUSSION

Electrophysiological Maturation and Synaptic Integration of the Genetically Modified Human Clones After Short-Term Grafting

The electrophysiological study of three groups of grafted hVM-NSC derivatives showed that the majority (93% of cells studied) were immature 6 weeks after grafting. These immature membrane properties are in line with reported cell membrane properties of human origin cells after their transplantation, and this agrees with the notion that longer times (minimum of 6 months) are required for human cells to mature after transplantation[16–18]. Nevertheless, all three groups showed RMPs in the range of what has been reported for in vitro nigral adult DA cells in rats[13,19].

The interesting finding in this study is that some cells did mature within such a short time span. This shows the potential of the hVM-NSCs to generate functional dopaminergic cells after grafting. This should be confirmed in future long-term studies, where cells will be allowed to mature 6 months to 1 year in in vivo grafts, where their mature phenotype will be assessed, along with behavioral effects.

Literature also shows that a given neuronal maturation stage may depend on the type of stem cell studied and/or the time that the cells are either maintained in culture or survive after grafting. For example, cocultured primary mouse VM neurospheres in organotypic cultures develop mature electrophysiological properties of DA neurons 3 weeks after grafting[12], while hiPSC-derived DA cells show limited maturation of their electrophysiological properties at 8 weeks in vitro[20].

To functionally assess the extent of integration of hVM1 cells and derivatives in the host tissue, we aimed at recording sPSCs at −70 mV in whole-cell voltage-clamp mode at 6 weeks following grafting (Fig. 6). Out of the 45 neurons recorded, 7 cells displayed sPSCs, thus proving that hVM1 cell derivatives are receiving synaptic inputs from other neurons, that is, that electrical communication exists. Since no spontaneous activity was recorded in the majority of the grafted cells, synaptic inputs are likely to come from the host. This would be in accordance with a recent study that, using the rabies virus as a monosynaptic tracer, demonstrates the existence of synaptic contacts between grafted embryonic cells and host cells at 6 weeks postgrafting[21].

TH Immunoreactivity and Behavioral Amelioration In Vivo

Only transplanted animals with C30-Bcl-X_L cells showed a significant reduction of drug-induced rotation. This behavioral amelioration remarks the proof of principle of the therapeutic efficacy of DA transplants for PD[1,2]. C30-Bcl-X_L cell derivatives produce the highest number of TH^+-immunoreactive cells after grafting. Likewise, the animals receiving C30-Bcl-X_L cells showed the highest spatial extension of TH^+ surviving cells in the caudate putamen, this being $5.05\pm0.9\%$. It has been previously reported that the extension of the caudate putamen receiving DA has to be higher than 4% in order to observe a behavioral amelioration at a similar time point[22]. Since in vitro grafting experiments show that the C30-Bcl-X_L cell derivatives are not functionally mature at 6 weeks, we hypothesize that the behavioral amelioration might be due to the C30-Bcl-X_L cells acting as biological dopaminergic pumps at this short-term stage. In line with the above, DA secreted by differentiated hVM-Bcl-X_L cell derivatives has been detected under in vitro conditions[7,23]. To confirm this, microdialysis experiments, which measure the DA concentrations in vivo, could be performed. Moreover, behavioral amelioration in the long term has been shown to depend on a previous graft integration and DA release[6]. It is worth noting that the total average number of TH^+ surviving cells in the transplanted group showing behavioral improvement ($462{,}741.67\pm233{,}802.38$) is in the range of what has been reported to be transplanted in fetal VM cell transplants, 450,000[24]. Although the final DA cells derived from these fetal transplants were not reported, micrografts covering extended extensions of the caudate putamen showed a motor recovery in the short term, an effect that was overall more prominent than the effect observed in single macrograft deposit experiments[24]. The above highlights the importance of migration of the grafted cells.

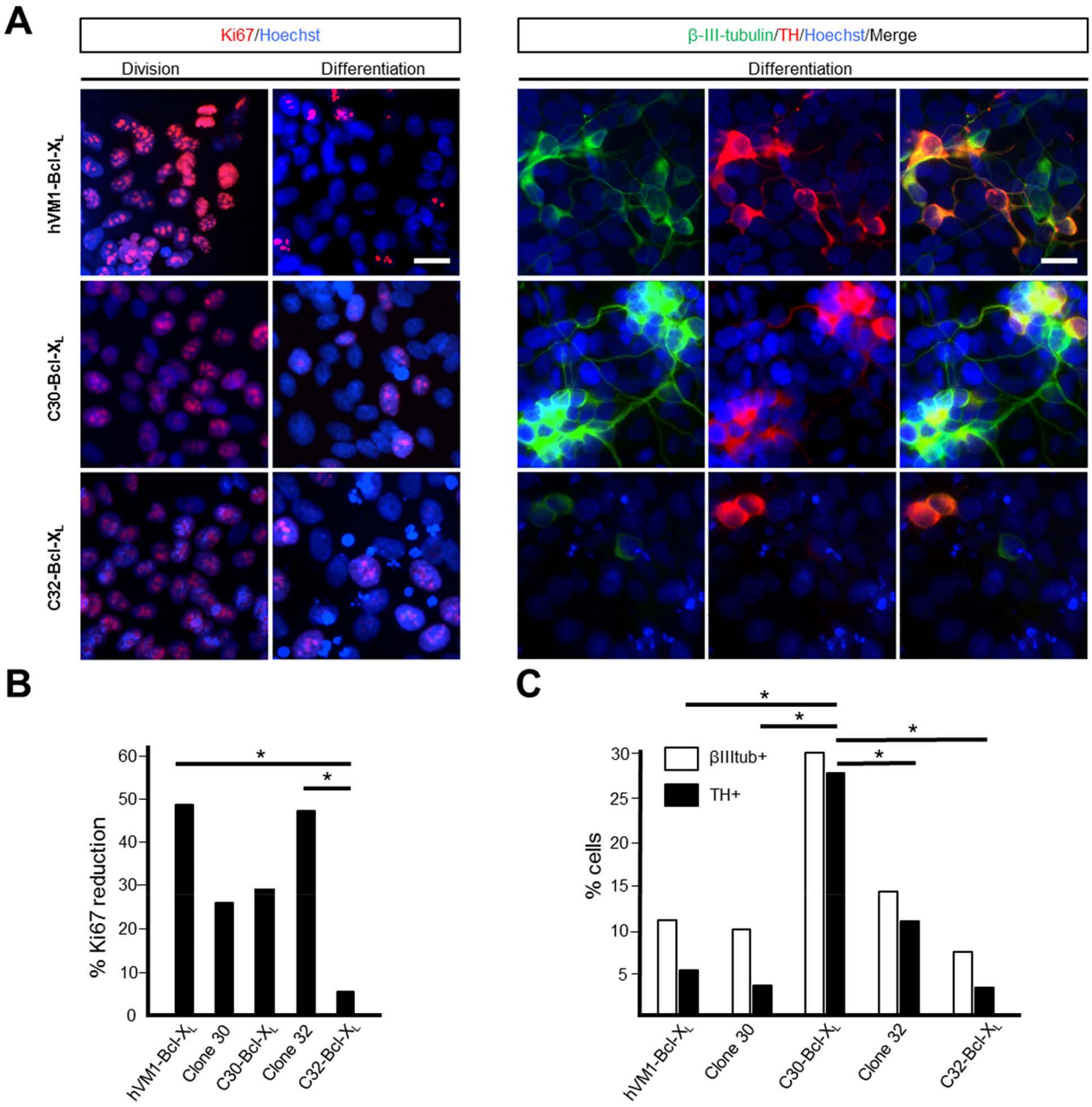

Figure 5. (A) Polyclonal hVM-Bcl-X_L cells and selected clones 30-Bcl-X_L and 32-Bcl-X_L were stained for Ki-67 or β-III-tubulin and TH under proliferation and 10 days under differentiation conditions. Scale bar: 20 μm for all microphotographs. (B) The graph represents the percentage reduction in the number of cells expressing Ki-67 after differentiation, using as reference the corresponding value under proliferation conditions ($p \leq 0.001$, Student's *t*-test). (C) The graph shows the percentage of neurons (β-III-tubulin$^+$) (empty bar) and, from those, the percentage becomes dopaminergic (TH$^+$) (black bar) after 10 days in vitro differentiation for the different cell lines ($p \leq 0.05$, Student's *t*-test; $n = 3$).

In addition to DA, glia-derived factors are also known to play a role in ameliorating drug-induced behavior in the short term[25,26]. These glia-derived factors can be secreted either by macrophages or microglia[25], by the host reactive astrocytes[26], or by the astrocytes derived from the grafted cells[7]. Glia-derived factors have been reported to neuroprotect and help in regenerating TH-immunoreactive fibers in parkinsonian models[27–29]. Our present results cannot exclude that secretion of glia-derived factors by different host cells and/or presence of auto-regenerated or nondegenerating host TH$^+$ fibers might have a synergistic effect in the observed behavioral amelioration.

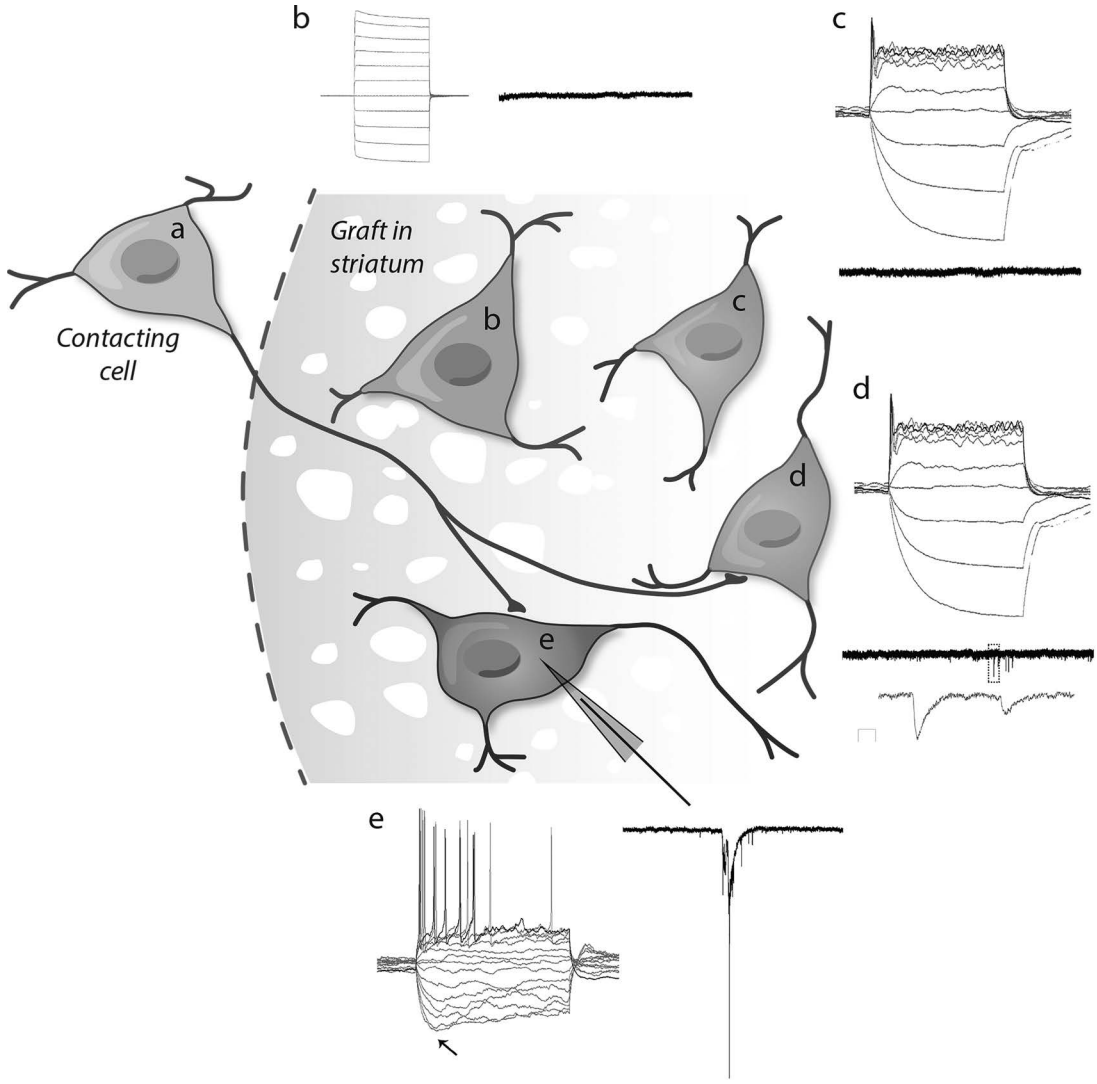

Figure 6. Schematics of hVM1-derived grafted cells showing different integration and biochemical maturation rates coexisting at the 6-week time point. (a) Contacting cell. (b) Immature GFP^+-grafted human cells do not receive inputs from the contacting cell and do not show any action potential (AP). A total of 26 cells with this phenotype were recorded. (c) Maturing human grafted cell starts expressing TH and shows a very immature AP but is not receiving any input from contacting cells either. A total of 12 cells with this phenotype were recorded. (d) Maturing cell expressing TH shows an immature AP and receives inputs from contacting cells. A total of four cells with this phenotype were recorded. (e) Integrated cell expressing TH shows characteristic dopaminergic action potentials with sag component (arrow). A total of three cells with this phenotype were recorded.

Interestingly, we did not observe major differences in the immune response between groups (Fig. 4A and B), and since animals transplanted with the clone giving low numbers of TH^+ cells and the sham group (Figs. 2A, D, and E, and 4E) have a nonsignificant behavioral improvement (Fig. 3A), our data strongly support the therapeutic efficacy of DA[1,2,30]. Moreover, we hypothesize that a significant amount of the DA involved in the amelioration should preferentially be secreted by the graft-derived DA cells, as there is a correlation between behavioral amelioration and presence of TH^+ cells (Fig. 3D), and low numbers of TH^+ cells do not induce any amelioration of the rotational behavior (Fig. 3A and E). Future experiments using optogenetics[6] and/or designer receptors exclusively activated by designer drug (DREADD)[31] systems to inhibit DA secretion from the graft-derived DA cells should help to unambiguously answer this question and also to determine the weight of the different components involved in the short-term amelioration.

Finally, the present results also show that although glial scar is dense, it still allows for communication between the host and the graft, tolerating migration of hNSCs through the neighboring parenchyma. It is known that the early events following the transplantation of embryonic

mesencephalic tissue grafted to an adult brain induce around them the formation of a glial scar and the upregulation of several extracellular matrix molecules[32]. The gliosis surrounding grafts of embryonic tissue is present during the time in which TH-immunoreactive neurites are growing from the dopaminergic neurons of the graft into the host brain[32]. This degree of gliosis is not sufficient to prevent axon growth from embryonic mesencephalic neurons[32], and based on recent publications it is likely that the glial scar can be helpful in cell axon regeneration[33].

Likewise, gliosis should be mild enough to allow cell migration for cells to cover big extensions of the caudate putamen. Long-term experiments (6 months to 1 year graft survival) are needed in order to answer if transplanted animals with human stem cell derivatives of C30-Bcl-X_L recover behavior because of a functional integration and if the glia scar can resolve after reinnervation is completed.

CONCLUSIONS AND FUTURE REMARKS

Although the majority of cells in the grafts are immature after 6 weeks under in vitro grafting conditions, animals receiving the more productive TH^+ cell line ameliorate rotational behavior at 7 weeks. The highest correlation with behavioral recovery in the short term is the extension of the caudate putamen that may be exposed to DA. Moreover, the present results are indicative of the potential of the hNSC-VM to generate functionally integrated dopaminergic cells after grafting. It remains to be studied if this functional integration and maturation of C30-Bcl-X_L derivatives in parkinsonian animals restore behavior in long-term experiments. Future long-term (up to 1 year) translational studies will address these issues in a design that will also allow to study neuron aging of graft maturation, graft-induced dyskinesia, toxicology, and safety.

ACKNOWLEDGMENTS: The authors thank the excellent technical support of Marta Gonzalez Mella, Pilar Santos Joven, Beatriz Garcia, and Beatriz Moreno (CBMSO); Prof. Zaal Kokaia and Dr. Cecilia Laterza (WNC) for their support and technical advice; Dr. Emmanuela Monni, Dr. Catherine Kitts, and UAM-SIdI for confocal microscopy assistance; and Dr. Bengt Mattson for his contribution to the graphics. This work was supported by the following grants: Kungliga Fysiografiska Sällskapet (to T.R.-M.); AFA Försäkring (100222) and VR Swedish Research Council (521-2012-2258) (to M.K.); and Spanish Ministry of Economy and Competitiveness (SAF2010-17167 and SAF2014-56101-R), Comunidad Autónoma Madrid (S2010-BMD-2336), and Instituto de Salud Carlos III (RETICS TerCel, RD12/0019/0013) (to A.M.-S.). This work was also supported by an institutional grant from Fundación Ramón Areces to the Center of Molecular Biology Severo Ochoa. Author contributions: A.M.-S.: Conception of the study, writing, reading, and editing of the article; M.P.P.: design of experiments, experimental procedures, and writing, reading, and editing of the article; N.A.: design, experimental procedures, and reading and editing of the article; A.N.: experimental procedures and reading of the article; M.K.: reading and editing of the article; T.R.-M.: conception of the study, design of experiments and experimental procedures, and writing, reading, and editing of the article. The authors declare no conflicts of interest.

REFERENCES

1. Politis M, Lindvall O. Clinical application of stem cell therapy in Parkinson's disease. BMC Med. 2012;10:1.
2. Lindvall O, Bjorklund A. Cell therapy in Parkinson's disease. NeuroRx 2004;1(4):382–93.
3. Lindvall O, Bjorklund A. Cell therapeutics in Parkinson's disease. Neurotherapeutics 2011;8(4):539–48.
4. Ramos-Moreno T, Lendinez JG, Pino-Barrio MJ, Del Arco A, Martinez-Serrano A. Clonal human fetal ventral mesencephalic dopaminergic neuron precursors for cell therapy research. PLoS One 2012;7(12):e52714.
5. Ramos-Moreno T, Castillo CG, Martinez-Serrano A. Long term behavioral effects of functional dopaminergic neurons generated from human neural stem cells in the rat 6-OH-DA Parkinson's disease model. Effects of the forced expression of BCL-X(L). Behav Brain Res. 2012;232(1):225–32.
6. Steinbeck JA, Choi SJ, Mrejeru A, Ganat Y, Deisseroth K, Sulzer D, Mosharov EV, Studer L. Optogenetics enables functional analysis of human embryonic stem cell-derived grafts in a Parkinson's disease model. Nat Biotechnol. 2015;33(2):204–9.
7. Courtois ET, Castillo CG, Seiz EG, Ramos M, Bueno C, Liste I, Martinez-Serrano A. In vitro and in vivo enhanced generation of human A9 dopamine neurons from neural stem cells by Bcl-XL. J Biol Chem. 2010;285(13):9881–97.
8. Villa A, Liste I, Courtois ET, Seiz EG, Ramos M, Meyer M, Juliusson B, Kusk P, Martinez-Serrano A. Generation and properties of a new human ventral mesencephalic neural stem cell line. Exp Cell Res. 2009;315(11):1860–74.
9. Liste I, Garcia-Garcia E, Martinez-Serrano A. The generation of dopaminergic neurons by human neural stem cells is enhanced by Bcl-XL, both in vitro and in vivo. J Neurosci. 2004;24(48):10786–95.
10. Liste I, Garcia-Garcia E, Bueno C, Martinez-Serrano A. Bcl-XL modulates the differentiation of immortalized human neural stem cells. Cell Death Differ. 2007;14(11):1880–92.
11. Lotharius J, Barg S, Wiekop P, Lundberg C, Raymon HK, Brundin P. Effect of mutant alpha-synuclein on dopamine homeostasis in a new human mesencephalic cell line. J Biol Chem. 2002;277(41):38884–94.
12. Tonnesen J, Parish CL, Sorensen AT, Andersson A, Lundberg C, Deisseroth K, Arenas E, Lindvall O, Kokaia M. Functional integration of grafted neural stem cell-derived dopaminergic neurons monitored by optogenetics in an in vitro Parkinson model. PLoS One 2011;6(3):e17560.
13. Grace AA, Onn SP. Morphology and electrophysiological properties of immunocytochemically identified rat dopamine neurons recorded in vitro. J Neurosci. 1989;9(10):3463–81.
14. Lammel S, Hetzel A, Hackel O, Jones I, Liss B, Roeper J. Unique properties of mesoprefrontal neurons within a dual mesocorticolimbic dopamine system. Neuron 2008;57(5):760–73.
15. Neuhoff H, Neu A, Liss B, Roeper J. I(h) channels contribute to the different functional properties of identified dopaminergic subpopulations in the midbrain. J Neurosci. 2002;22(4):1290–302.

16. Brundin P, Strecker RE, Widner H, Clarke DJ, Nilsson OG, Astedt B, Lindvall O, Bjorklund A. Human fetal dopamine neurons grafted in a rat model of Parkinson's disease: Immunological aspects, spontaneous and drug-induced behaviour, and dopamine release. Exp Brain Res. 1988;70(1):192–208.
17. Winkler C, Kirik D, Bjorklund A. Cell transplantation in Parkinson's disease: How can we make it work? Trends Neurosci. 2005;28(2):86–92.
18. Avaliani N, AT SR, Ledri M, Bengzon J, Koch P, Brustle O, Deisseroth K, Andersson M, Kokaia M. Optogenetics reveal delayed afferent synaptogenesis on grafted human induced pluripotent stem cell-derived neural progenitors. Stem Cells 2014;32(12):3088–98.
19. Bloom FE, Kupfer DJ. Psychopharmacology—4th generation of progress. 4th ed. New York (NY): Raven Press; 1995.
20. Hartfield EM, Yamasaki-Mann M, Ribeiro Fernandes HJ, Vowles J, James WS, Cowley SA, Wade-Martins R. Physiological characterisation of human iPS-derived dopaminergic neurons. PLoS One 2014;9(2):e87388.
21. Grealish S, Heuer A, Cardoso T, Kirkeby A, Jonsson M, Johansson J, Bjorklund A, Jakobsson J, Parmar M. Monosynaptic tracing using modified rabies virus reveals early and extensive circuit integration of human embryonic stem cell-derived neurons. Stem Cell Reports 2015; 4(6):975–83.
22. Leone P, McPhee SW, Janson CG, Davidson BL, Freese A, During MJ. Multi-site partitioned delivery of human tyrosine hydroxylase gene with phenotypic recovery in Parkinsonian rats. Neuroreport 2000;11(6):1145–51.
23. Amato L, Heiskanen A, Caviglia C, Shah F, Zor K, Skolimowski M, Madou M, Gammelgaard L, Hansen R, Seiz EG, Ramos M, Ramos Moreno T, Martinez-Serrano A, Keller SS, Emneus J. Pyrolysed 3D-carbon scaffolds induce spontaneous differentiation of human neural stem cells and facilitate real-time dopamine detection. Adv Funct Mater. 2014;24(44):10.
24. Nikkhah G, Duan WM, Knappe U, Jodicke A, Bjorklund A. Restoration of complex sensorimotor behavior and skilled forelimb use by a modified nigral cell suspension transplantation approach in the rat Parkinson model. Neuroscience 1993;56(1):33–43.
25. Batchelor PE, Liberatore GT, Wong JY, Porritt MJ, Frerichs F, Donnan GA, Howells DW. Activated macrophages and microglia induce dopaminergic sprouting in the injured striatum and express brain-derived neurotrophic factor and glial cell line-derived neurotrophic factor. J Neurosci. 1999;19(5):1708–16.
26. Asada H, Ip NY, Pan L, Razack N, Parfitt MM, Plunkett RJ. Time course of ciliary neurotrophic factor mRNA expression is coincident with the presence of protoplasmic astrocytes in traumatized rat striatum. J Neurosci Res. 1995;40(1):22–30.
27. Rosenblad C, Martinez-Serrano A, Bjorklund A. Intrastriatal glial cell line-derived neurotrophic factor promotes sprouting of spared nigrostriatal dopaminergic afferents and induces recovery of function in a rat model of Parkinson's disease. Neuroscience 1998;82(1):129–37.
28. Oiwa Y, Yoshimura R, Nakai K, Itakura T. Dopaminergic neuroprotection and regeneration by neurturin assessed by using behavioral, biochemical and histochemical measurements in a model of progressive Parkinson's disease. Brain Res. 2002;947(2):271–83.
29. Drinkut A, Tereshchenko Y, Schulz JB, Bahr M, Kugler S. Efficient gene therapy for Parkinson's disease using astrocytes as hosts for localized neurotrophic factor delivery. Mol Ther. 2012;20(3):534–43.
30. Lu L, Zhao C, Liu Y, Sun X, Duan C, Ji M, Zhao H, Xu Q, Yang H. Therapeutic benefit of TH-engineered mesenchymal stem cells for Parkinson's disease. Brain Res Brain Res Protoc. 2005;15(1):46–51.
31. Dell'Anno MT, Caiazzo M, Leo D, Dvoretskova E, Medrihan L, Colasante G, Giannelli S, Theka I, Russo G, Mus L, Pezzoli G, Gainetdinov RR, Benfenati F, Taverna S, Dityatev A, Broccoli V. Remote control of induced dopaminergic neurons in parkinsonian rats. J Clin Invest. 2014;124(7):3215–29.
32. Barker RA, Dunnett SB, Faissner A, Fawcett JW. The time course of loss of dopaminergic neurons and the gliotic reaction surrounding grafts of embryonic mesencephalon to the striatum. Exp Neurol. 1996;141(1):79–93.
33. Anderson MA, Burda JE, Ren Y, Ao Y, O'Shea TM, Kawaguchi R, Coppola G, Khakh BS, Deming TJ, Sofroniew MV. Astrocyte scar formation aids central nervous system axon regeneration. Nature 2016;532(7598):195–200.